PHYSICAL REVIEW B VOLUME 1, NUMBER 12 15 JUNE 1970

Energy Bands of Hexagonal NiS†

J. M. Tyler* and J. L. Fry
Department of Physics and Astronomy, Louisiana State University, Baton Rouge, Louisiana 70803
(Received 14 January 1970)

Energy bands are calculated for hexagonal NiS using lattice constants and crystal potential appropriate to the metallic phase. Group theoretic results for s, p, and d bands in the NiAs structure are obtained, and the calculation is performed using a first-principles tight-binding method. The energy band structure is characterized by a $3d$ band about 3 eV wide, hybridized with a broad s-p band, indicating s-d-type conductivity. The Fermi energy lies just below the top of the d bands and the density of states exhibits a strong sharp peak about 1 eV below the Fermi energy. Since the energy bands suggest considerable structure in the low-energy region of the reflectivity, selection rules, polarizations, and energies for some of the spectra are presented. The band structure is discussed in terms of the metal-to-semiconductor transition which has been observed for hexagonal NiS.

I. INTRODUCTION

This paper reports an energy band calculation for the metallic phase of hexagonal NiS. NiS crystallizes in the NiAs structure, which is common for binary compounds of transition metals,[1] yet there have been no calculations for these compounds owing to the difficulty in performing first-principles calculations for this structure, and because of the lack of experimental data needed to perform simpler pseudopotential calculations. This paper appears to be the first attempt to perform a band calculation in the NiAs crystal structure.

Transition metal compounds have long presented difficulties to band theory, but their wide variety of electric and magnetic properties make them both interesting and challenging. The extent to which band theory alone can account for properties of these compounds has not been determined, and is the subject of some controversy.[2] The most famous example of the apparent failure of band theory is NiO.[3-6] Although it is certain that band theory must be corrected in some instances, such as NiO, it is not clear just how it can best be adapted to account for essential features of the electronic correlations which are responsible for its failure. Clear cut decisions must await reliable data on good crystals, which are not available for most of these compounds. Interpretation of data from these compounds is confused by experimental problems of defects, impurities, nonstoichiometry, and mixed phases. However, substantial advances have been made in recent years, so band calculations are useful at this time. Data available and the report of a metal-to-semiconductor transition[7] have motivated the choice of NiS for this investigation.

In order to yield reasonable results for transition metal compounds, band theory must provide a computational method which can adequately treat both the broad and narrow bands which are present, while using a realistic crystalline potential. Corrections to muffin-tin potentials have been found to be important in the case of ReO_3,[8] and are presumably important in all the transition metal compounds. An additional difficulty in the NiAs structure is the presence of two molecules per unit cell, so that the number of bands is large. This complicates orthogonalized-plane-wave (OPW) calculations because of the large number of core orthogonalizations required, while in augmented-plane-wave (APW) calculations it slows the rate of convergence of the APW expansion considerably,[8] and in tight-binding calculations it increases the size of the minimal basis set. The tight-binding method has been chosen for this study.

The remainder of this paper is organized as follows. In Sec. II the experimental information available for NiS is reviewed. Section III describes the method of calculation and discusses some group theoretic results for the NiAs structure which are used in the band calculations. Energy bands, density of states, and optical transitions are presented and discussed in Sec. IV. In Sec. V the metal-to-semiconductor transition is discussed in terms of the energy bands presented in Sec. IV. Section VI contains concluding remarks.

II. EXPERIMENTAL INFORMATION

The properties of NiS are summarized by Adler[2] and by Sparks and Komoto.[9] A brief review is presented in this section.

Above 620 °K NiS crystallizes in the NiAs structure, space group D_{6h}^4. When cooled slowly, a crystallographic phase change occurs in which two different phases appear to coexist. However, if quenched from above 620 °K to room tempera-

ture, the NiAs structure is retained. Upon further cooling, the c and a axes shrink slowly, but at 264 °K an abrupt discontinuity occurs in both lattice constants, c increasing by about 1% and a by about 0.3%.[10] There is a simultaneous transition from metal-to-semiconductor,[7] accompanied by an antiferromagnetic alignment of spins along the c axis forming a hexagonal layer structure[10] of spins characterized by ferromagnetic coupling within layers and antiferromagnetic coupling between adjacent layers, as shown in Fig. 1, which is a unit cell for the NiAs structure. This situation persists down to 4 °K with no distortion from the NiAs structure detected. Upon warming back through the transition, a hysteresis is observed in resistivity, magnetic susceptibility, and lattice parameters, indicating that the transition is first order. The width of the transition is about 3°.

Resistivity measurements show characteristic semiconducting behavior with activation energy of about 0.12 eV just below the transition, while above the transition temperature there is metallic resistivity with a positive temperature coefficient: $\rho(T)/\rho(0\,^\circ\mathrm{C}) = 0.76 + 6.8 \times 10^4 T$ (T in °K).[11] Through the transition the resistivity jumps by a factor of 40. The transition temperature and width of the transition depend sensitively upon stoichiometry, excess sulfur causing substantial lowering and broadening: $T_c = (75 \pm 15)$ °K for 3% excess sulfur. An early report[12] of a Néel temperature at 150 °K presumably corresponds to about 2% excess sulfur in the samples used.

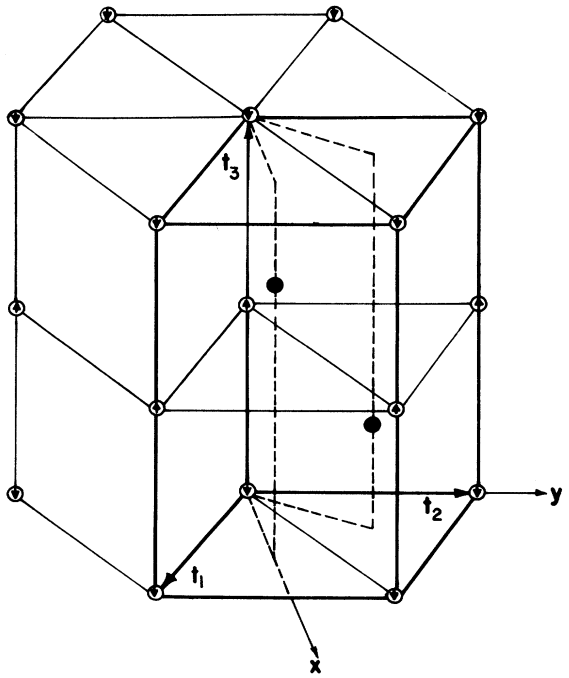

FIG. 1. Unit cell for the NiAs crystal structure. Open circles are nickel atoms, dark circles arsenic atoms. Arrows on the nickel atoms shown spin arrangement for semiconducting NiS.

Neutron diffraction studies of NiS yield a magnetic moment of $(1.66 \pm 0.08)\mu_B$ at 4.2 °K and $(1.50 \pm 0.10)\mu_B$ at 260 °K, so that just below the transition temperature sublattice magnetization is 90% saturated. Above T_N the magnetic moment for nickel atoms is less than $0.5\mu_B$, as deduced from the absence of paramagnetic diffuse scattering.[13] Studies of NiS under pressure show a large negative pressure dependence of the Néel temperature: $dT_N/dp = (-6.0 \pm 0.3)$°/kbar,[14] and neutron diffraction studies of NiS under pressure show a small, almost temperature-independent compressibility.[15]

There have been no optical studies of NiS, for which good single crystals are desired. Single crystals tend to crack on undergoing the phase transition; this difficulty must be overcome for optical studies. Likewise, there have been no Fermi-surface studies on metallic NiS. Furthermore, these seem to be out of the question due to the high temperatures and short mean free paths in the metallic phase. However, it might be possible to get Fermi-surface information from positron annihilation which can be done above 265 °K.

III. DETAILS OF CALCULATION

A. Method

The tight-binding method has been used in this calculation. The method will not be described in detail here, since adequate discussions are given elsewhere.[16-18] The particular version of tight binding used in this paper has also been discussed elsewhere.[19,20]

The electronic wave function in the crystal is expanded in a set of Bloch functions constructed in the usual manner:

$$b_{nlm}(\vec{k}, \vec{r}, \vec{\tau}_i) = \frac{1}{\sqrt{N}} \sum_\nu e^{i\vec{k}\cdot(\vec{R}_\nu + \vec{\tau}_i)} \psi_{nlm}(\vec{r} - \vec{R}_\nu - \vec{\tau}_i), \quad (1)$$

where N is the number of sites in the crystal and the summation is carried out over all N of these sites $\vec{R}_\nu$. Here $\vec{\tau}_i$ is the position (in the cell at the origin) of the ith type of atom with electronic wave function ψ_{nlm}, where nlm are the usual atomic quantum numbers. It is convenient to form linear combinations of these ψ_{nlm} which have special transformation properties under the group of the wave vector $\vec{k}$ before performing the Bloch sum in Eq. (1). The appropriate combinations are described below. Energy bands are obtained by taking matrix elements of the one-electron Hamiltonian between these functions, and solving the secular equation

$$| H_{ij}(\vec{k}) - ES_{ij}(\vec{k}) | = 0 , \tag{2}$$

where i stands for the labels nlm and $\vec{\tau}_i$, and $H = -\nabla^2 + V(\vec{r})$. The overlap, kinetic-energy, and potential-energy matrix elements are given by

$$\begin{aligned} S_{ij}(\vec{k}) &= \exp[i\vec{k}\cdot(\vec{\tau}_j - \vec{\tau}_i)] \textstyle\sum_\nu \exp[i\vec{k}\cdot\vec{R}_\nu \\ &\quad \times \langle \psi_{nlm}(\vec{\tau}_i) \mid \psi_{n'l'm'}(\vec{R}_\nu + \vec{\tau}_j)\rangle] , \\ T_{ij}(\vec{k}) &= \exp[i\vec{k}\cdot(\vec{\tau}_j - \vec{\tau}_i)] \textstyle\sum_\nu \exp[i\vec{k}\cdot\vec{R}_\nu \\ &\quad \times \langle \psi_{nlm}(\vec{\tau}_i) \mid -\nabla^2 \mid \psi_{n'l'm'}(\vec{R}_\nu + \vec{\tau}_j)], \\ V_{ij}(\vec{k}) &= \exp[i\vec{k}\cdot(\vec{\tau}_j - \vec{\tau}_i)] \textstyle\sum_\nu \exp[i\vec{k}\cdot\vec{R}_\nu \\ &\quad \times \langle \psi_{nlm}(\vec{\tau}_i) \mid v(\vec{r}) \mid \psi_{n'l'm'}(\vec{R}_\nu + \vec{\tau}_j)]. \end{aligned} \tag{3}$$

The overlap and kinetic-energy integrals are two-center integrals and may be evaluated by standard techniques.[21,22] The potential-energy integrals are three-center integrals and are far more difficult to evaluate; it is the intractability of these potential integrals which has heretofore forced what often turned out to be drastic approximations in applying the method of tight binding. Until recently, the tight-binding scheme has been used primarily as an interpolation scheme to fit more accurate calculations, or used as the basis for pseudopotential calculations. The method used here for evaluating these three-center integrals requires analytic expressions for the atomic wave functions in the form of sums of Slater-type orbitals, and a Fourier-series expression for the crystal potential.[19,20] For this calculation the analytic wave functions for neutral atoms of nickel ($3d^8 4s^2$) and sulfur ($3p^4$) were obtained from Clementi's tables.[23] The crystal potential was generated from the same wave functions.

B. Crystal Potential

The Coulomb part of the crystal potential was constructed as a superposition of spherically averaged atomic potentials, so that, with analytic wave functions, the Fourier coefficients could be written explicitly. Since NiS has a center of inversion, the Fourier series may be written as

$$V(\vec{r}) = \textstyle\sum_n V(\vec{k}_n)\cos(\vec{k}_n\cdot\vec{r}), \tag{4}$$

$$\text{with} \quad V(\vec{k}_n) = \frac{1}{N\Omega_0}\int V(\vec{r}) e^{i\vec{k}_n\cdot\vec{r}} d^3r , \tag{5}$$

where Ω_0 is the volume of the unit cell and $\vec{k}_n$ are the hexagonal reciprocal-lattice vectors and the integral is over all space. Noting that there are two molecules per unit cell, the superposition of atomic potentials is

$$\begin{aligned} V(\vec{r}) = \textstyle\sum_\nu & V_{Ni}(\vec{r} - \vec{R}_\nu - \vec{\tau}_1) + V_{Ni}(\vec{r} - \vec{R}_\nu - \vec{\tau}_2) \\ & + V_S(\vec{r} - \vec{R}_\nu - \vec{\tau}_3) + V_S(\vec{r} - \vec{R}_\nu - \vec{\tau}_4), \end{aligned} \tag{6}$$

where V_{Ni} and V_S are the spherically averaged atomic potentials for nickel and sulfur. Changing variables in each integral of Eq. (5) and performing the sum over ν,

$$\begin{aligned} V(\vec{k}_n) = \frac{1}{\Omega_0}[& \exp(-i\vec{k}_n\cdot\vec{\tau}_i)\int V_{Ni}(\vec{r})\exp(-i\vec{k}_n\cdot\vec{r})d^3r \\ & + \exp(-i\vec{k}_n\cdot\vec{\tau}_2)\int V_{Ni}(\vec{r})\exp(-i\vec{k}_r\cdot\vec{r})d^3r \\ & + \exp(-i\vec{k}_n\cdot\vec{\tau}_3)\int V_S(\vec{r})\exp(-i\vec{k}_n\cdot\vec{r})d^3r \\ & + \exp(-i\vec{k}_n\cdot\vec{\tau}_4)\int V_S(\vec{r})\exp(-i\vec{k}_n\cdot\vec{r})d^3r], \end{aligned} \tag{7}$$

where the integrals are taken over all space. Using the spherically averaged potentials, these integrals may be written

$$\begin{aligned} \int V_{Ni}(\vec{r})\exp(-i\vec{k}_n\cdot\vec{r})d^3r = & -\frac{224\pi}{|\vec{k}_n|^2} + \frac{8\pi}{|\vec{k}_n|^3} \\ & + \textstyle\sum_n N(nl)\int_0^\infty |U_{nl}(r)|^2 r\sin k_n r\, dr , \end{aligned} \tag{8}$$

where $N(nl)$ is the occupation of the atomic state nl and U_{nl} is the radial part of the atomic orbital for that state. Throughout this paper atomic units are used, with energy measured in Ry. For Clementi's wave functions the integrals are elementary, although the number of terms involved makes them useful for computer calculation only. A similar expression holds for the sulfur integral.

The Fourier coefficient for $\vec{k}_n = 0$ must be calculated separately by a limiting process, and for nickel the integral is

$$\begin{aligned} \lim_{k_n\to 0}\int & V_{Ni}(\vec{r})\exp(-i\vec{k}_n\cdot\vec{r})d^3r \\ & = -\frac{4\pi}{3}\textstyle\sum_{nl} N(nl)\int_0^\infty |U_{nl}(r)|^2 r^4 dr, \end{aligned} \tag{9}$$

and similarly for sulfur.

A $\rho^{1/3}$ exchange potential of the type proposed by Slater[24] was used in this calculation. Fourier coefficients of this exchange potential were calculated by obtaining a spherical average of the crystal charge density about each atom in the unit cell and performing the integrals of $\rho(r)^{1/3}$ over atomic spheres with radius half the nearest-neighbor distance, combining them as indicated in Eq. (7). The average value of this potential in the interstitial region was -0.4 Ry. The exchange potential integrals were multiplied by an adjustable parameter λ when constructing matrix elements, so that variations in the exchange potential could be investigated.

Some comment on the Fourier-series expres-

sion for the crystal potential is appropriate at this point. From Eq. (8) the large k dependence of the Fourier coefficients is $1/k^2$ and the series (4) will not converge after any finite number of terms. This, of course, is due to the nuclear point charges located at atomic sites, so this part of the potential is the Fourier equivalent to a Madelung potential. Since the atoms are assumed to be in a neutral configuration in this calculation, there is no difficulty with convergence of the other series expression (6), contrary to what is found in ionic crystals. The solution to this problem for the ionic case is given by Ewald,[25] but for the present purposes it is sufficient to observe that it is not the series but integrals with the series (4) which appear in this calculation. Integrals involving atomic function centered on different sites have additional factors $\exp(-k_n R)$, where R is the separation of the centers, so convergence of these integrals is quite good. For crystal field integrals (two wave functions on the same atom), the Fourier series for the integral converges more slowly, coefficients for the integral are inversely proportional to $(\alpha^2+k^2)^2k^2$ for large k, where α is the sum of two of the Slater exponential parameters. Convergence of this sum is slower for more localized functions, i.e., the deep core functions. On the other hand, these crystal field integrals are only two-center integrals and may be evaluated directly instead of with the Fourier series, if convergence is not rapid enough. Although it was not necessary to sum the Fourier series (4) in this calculation, it was useful to compare (4) and (6) to check that Fourier coefficients had been obtained correctly. This was done by comparing contributions from electrons only, which eliminated the simple, but troublesome, term in (4).

One further comment about the Fourier series (4): In the tight-binding method the time consuming task is evaluation of the three-center integrals. These can be evaluated once for a given set of atomic wave functions for each value of R_ν and k_n and saved. The potential can then be adjusted to self-consistency merely by recalculating the Fourier coefficients and regenerating the band structure, without spending the time to calculate integrals, since they remain the same. Of course, if some or all of the Slater exponents are adjusted variationally, the integrals must be recomputed. However, for a reasonable choice of starting atomic orbitals it is likely that improvements of this type are unimportant compared to improvements which need to be made in the treatment of other solid-state effects, especially exchange interactions in the transition metal compounds.

C. Crystal Structure

The NiS crystal structure, belonging to a nonsymmorphic space group D_{6h}^4, specifies the direct lattice vectors, reciprocal-lattice vectors, and atomic positions $\vec{\tau}_i$ in the unit cell which appear in expressions for the crystal potential. A unit cell is shown in Fig. 1 for NiS, which may be viewed as a simple hexagonal nickel lattice interpenetrating with a hexagonal close-packed lattice of sulfur atoms. The lattice constants used in this calculation were $a = 6.5064$ and $c = 10.046$, in atomic units, corresponding to values observed just above the transition temperature.[10] The primitive vectors for the direct lattice $\vec{t}_i$ and reciprocal lattice $\vec{b}$ are

$$\begin{aligned} \vec{t}_1 &= \tfrac{1}{2}a(\sqrt{3}\vec{i}-\vec{j}), & \vec{b}_1 &= (4\pi/\sqrt{3}a)\vec{i} \\ \vec{t}_2 &= a\vec{j}, & \vec{b}_2 &= (2\pi/\sqrt{3}a)(\vec{i}+\sqrt{3}\vec{j}), \\ \vec{t}_3 &= c\vec{k}, & \vec{b}_3 &= (2\pi/c)\vec{k}, \end{aligned} \tag{10}$$

where $\vec{i}$, $\vec{j}$, $\vec{k}$ are unit vectors along the x, y, and z coordinate axes. Locations of the atoms within the unit cell are given in terms of these primitive vectors. For NiS (NiAs structure) there are nickel atoms at $\vec{\tau}_1 = (0, 0, 0)$ and $\vec{\tau}_2 = (0, 0, \frac{1}{2})$, and sulfur atoms at $\vec{\tau}_3 = (\frac{1}{3}, \frac{2}{3}, \frac{1}{4})$ and $\vec{\tau}_4 = (\frac{2}{3}, \frac{1}{3}, \frac{3}{4})$. Using these nonprimitive position vectors and defining a reciprocal-lattice vector by $\vec{k}_n = n_1\vec{b}_1 + n_2\vec{b}_2 + n_3\vec{b}_3$, the structure factors in (7) may be written explicitly and the Fourier coefficients of the potential become, for n_3 even,

$$\begin{aligned} V(\vec{k}_n) = \frac{2}{\Omega_0}\Bigg(& \int V_{\mathrm{Ni}}(\vec{r})\exp(-i\vec{k}_n\cdot\vec{r})\,d^3r \\ & + (-1)^{(2n_1+2n_2+n_3)/2}[\cos\tfrac{1}{3}\pi(n_1-n_2)] \\ & \times\int V_{\mathrm{S}}(\vec{r})\exp(-i\vec{k}_n\cdot\vec{r})\,d^3r\Bigg), \end{aligned} \tag{11}$$

and, for n_3 odd,

$$\begin{aligned} V(\vec{k}_n) = -\frac{2}{\Omega_0}(-1)^{(2n_1+2n_2+n_3+1)/2}[\sin\tfrac{1}{3}\pi(n_1-n_2)] \\ \times\int V_{\mathrm{S}}(\vec{r})\exp(-i\vec{k}_n\cdot\vec{r})\,d^3r, \end{aligned} \tag{12}$$

where the integrals are given by Eq. (8) for nickel and a similar equation for sulfur.

For n_3 odd there are sulfur contributions to $V(\vec{k}_n)$ but not nickel contributions, because there exists reflection symmetry through the plane $Z = 0$ for nickel atoms, but not for sulfur atoms. Less apparent symmetries for the NiAs structure and for the space group D_{6h}^4 are discussed by Slater,[26] who gives operations of the group and tables of irreducible representations. Using standard group theoretic techniques it is possible to block diagonalize the Hamiltonian and overlap matrices and factor the secular determinant (2) by forming linear combinations of the tight-binding

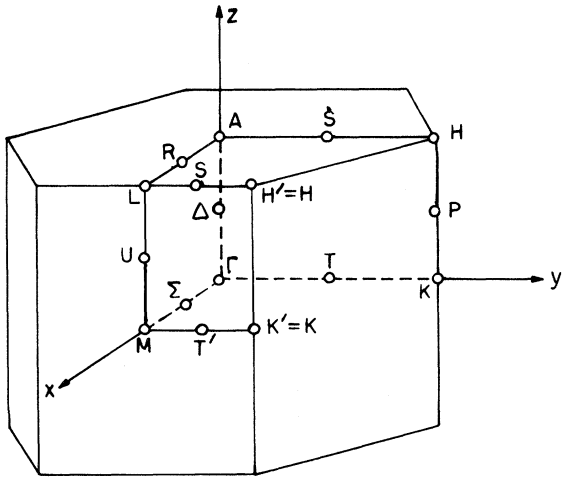

FIG. 2. Brillouin zone for hexagonal space group D_{6h}^4, with symmetry points and lines labeled after Herring (Ref. 27).

basis functions (1) which transform like rows of these irreducible representations. This has been done for NiS at points and lines of symmetry in the Brillouin zone which are shown in Fig. 2, where the standard labels of Herring[27] have been used. The linear combinations were obtained by a projection operator technique, using matrix elements for the irreducible representations found in Slater's book.[26] Presence of nonprimitive translations in some of the operations of this nonsymmorphic space group complicated these procedures as well as other group theoretic procedures for this crystal. Symmetrized combinations of atomic orbitals for the NiS crystal are given in the Appendix. These combinations show which atomic functions (s, p, d) on each atom in the unit cell transform according to each of the irreducible representations of the group of the wave vector, and which, therefore, are coupled by the crystal Hamiltonian. This information is very useful in interpreting results of the energy band calculation and comparing with crystal field and molecular orbital models previously proposed.

IV. RESULTS OF BAND CALCULATION

A. Energy Bands

Energy bands were first calculated using 4s and 3d orbitals from nickel and 3p orbitals from sulfur. Since there are two atoms of each type in the unit cell, this required a secular determinant with a complex 18×18 matrix. Energy eigenvalues in the vicinity of the Fermi energy at points and lines of symmetry in the Brillouin zone are shown in Figs. 3 and 4, where the exchange parameter λ was chosen as 1.0, corresponding to Slater's original exchange potential. Figure 5 shows energy bands along the Σ axis for λ = 0.85, a value used in band calculations for Ni.[28]

When constructing matrix elements given by Eq. (3), care was taken to obtain convergence in the sum over lattice vectors. Convergence of this sum was slowest for integrals involving s functions, so to ensure convergence, 38th neighbors were summed for s-s integrals, 18th neighbors for s-d, and 19th for s-p. Similar precautions were taken in the reciprocal-lattice sums in Eq. (4). With respect to these sums, energy bands given in this paper are believed converged

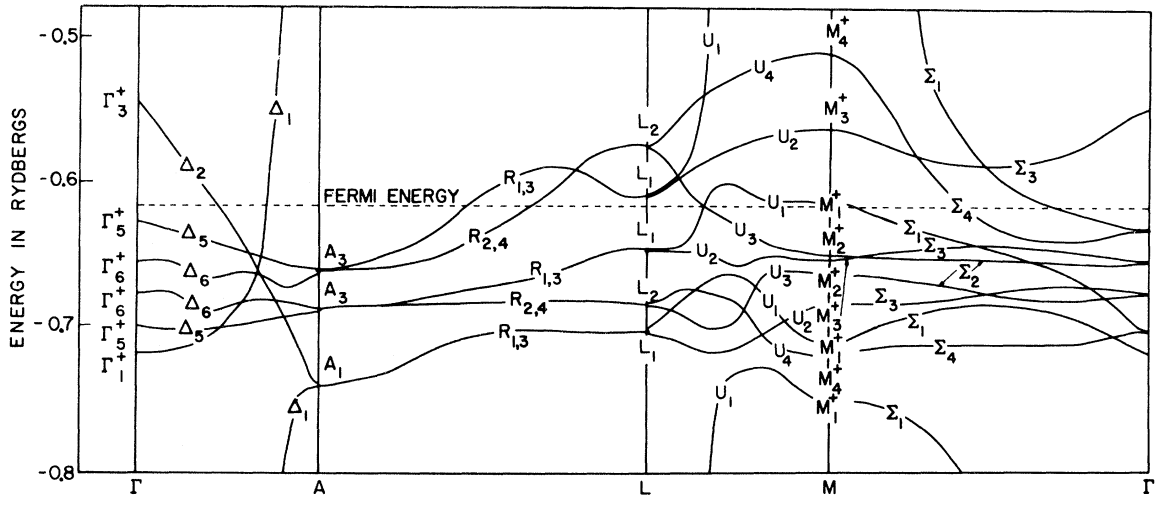

FIG. 3. Energy bands for metallic NiS.

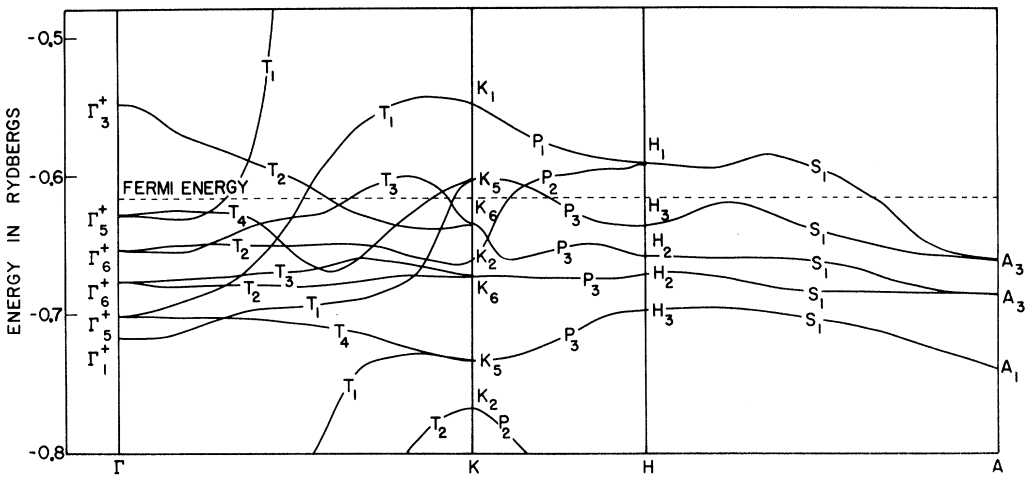

FIG. 4. Energy bands for metallic NiS.

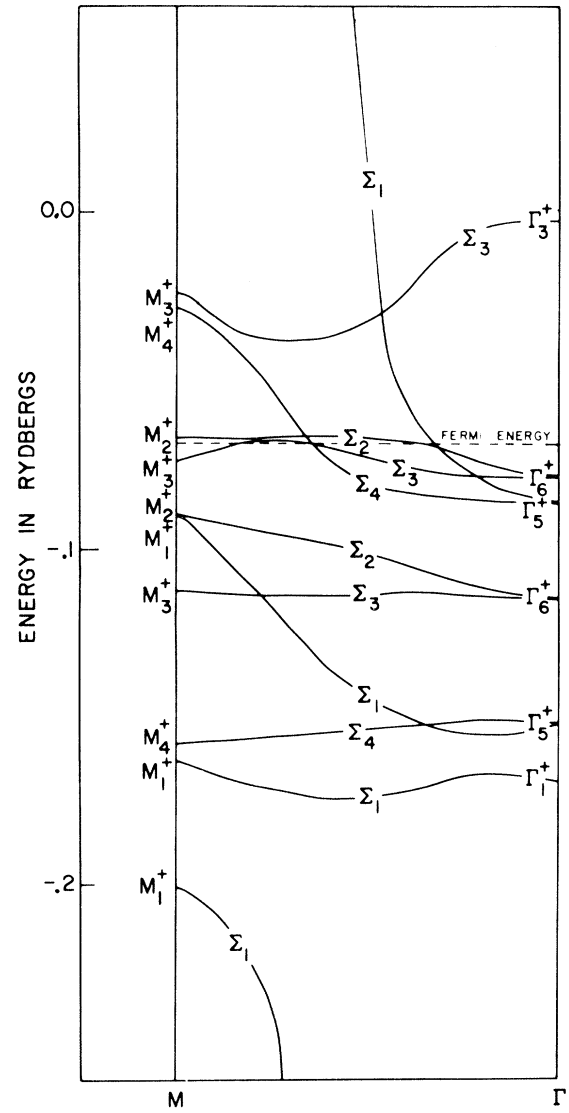

FIG. 5. Energy bands along the Σ axis for exchange parameter $\lambda = 0.85$.

to within an accuracy of at least 0.001 Ry.

In this tight-binding calculation the entire set of Slater-type orbitals (STO) used by Clementi to expand the atomic functions were included in the analytic form of the atomic wave functions, which resulted in additional sums in matrix elements and further lengthening of the calculation. It might be possible to use a truncated set of STO basis functions for the atom, as was done in a calculation of the energy bands of metallic lithium,[19] but results of calculations in Ni[28] and MnS[29] indicate that choice of atomic wave functions may be important. In fact, it should be noted that the Hartree-Fock linear combination of STO's given by Clementi may not be the best combination of these orbitals for the solid, and it may be desirable to use the entire STO basis set in the solid instead of that linear combination which satisfies the variational principle for the atom. With the method of obtaining the integrals used here, no additional work would be required to evaluate integrals of STO's, although the size of the secular determinate would be increased accordingly. Since this calculation was the first attempt to understand the band structure of NiS, the smaller determinate (complex) was preferred for calculational convenience.

B. Comparison with MnAs

Although there are no theoretical or experimental determinations of the band structure of other transition metal compounds with the NiAs crystal structure with which this work may be compared, Goodenough[30] has proposed a model to interpret the magnetic properties of MnAs, both in the hexagonal phase and orthorhombic phase. His model is based upon molecular orbital theory, which has been the traditional approach to the

theory of transition metal compounds.[31] To explain the phase transitions which occur in MnAs, he invoked the concept of a critical distance R_c, such that for Mn-Mn nearest-neighbor distances $R > R_c$ manganese d electrons behave as localized electrons, while for $R < R_c$ they behave as collective, or band electrons. He further assumed that the d bands and Fermi energy fall in the gap between s-p bonding and antibonding bands, with four d electrons per manganese ion occupying orbitals a_1^T, e^T, and e, which are identified in this work with $Z^2(\vec{\tau}_1) \pm Z^2(\vec{\tau}_2)$; $XY(\vec{\tau}_1) + XY(\vec{\tau}_2)$ and $[X^2(\vec{\tau}_1) - Y^2(\vec{\tau}_1)] \pm [X^2(\vec{\tau}_2) - Y^2(\vec{\tau}_2)]$; and $YZ(\vec{\tau}_1) \pm YZ(\vec{\tau}_2)$ and $ZX(\vec{\tau}_1) \pm ZX(\vec{\tau}_2)$ orbitals, respectively. According to his model [Fig. 6(a)], the a_1^T and e bonding and antibonding orbitals form collective bands, while e^T bonding and antibonding orbitals represent localized electrons, which follows from the observation that the hexagonal lattice constant are such that $R_1 = c/2 < R_c \approx 3.7$ Å, and $R_2 = a > R_c$. The a_1^T bands were assumed most stable (lowest in energy) followed by very narrow e^T bands (localized), with the collective e bands highest in energy. The magnetic moment 3.1 μ_B was explained by an exchange splitting, so that the four d electrons per manganese ion filled a_1^T and e^T for α spin, but filled only $\frac{1}{4}$ of the e band of α spin (i.e., $\frac{1}{2}$ electron per manganese atom) and $\frac{1}{2}$ of the $a_1^T\beta$ spin band.

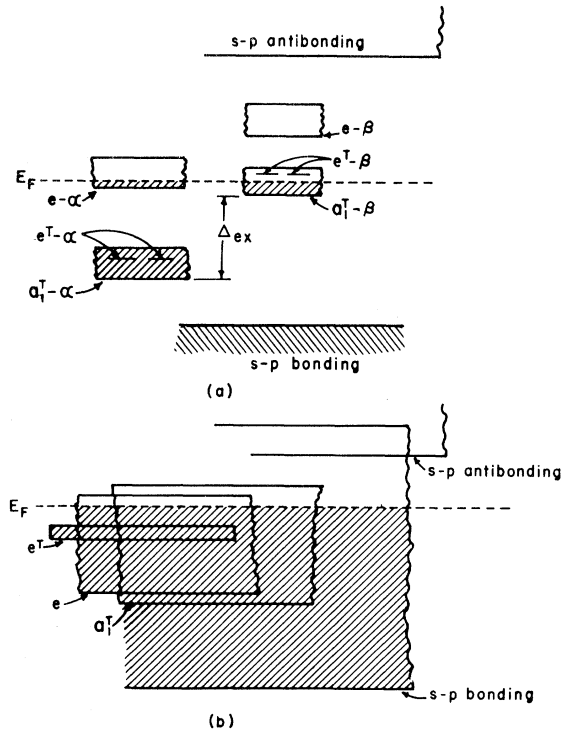

FIG. 6. (a) Band model for MnAs, after Goodenough *et al.* (Ref. 30). The bands labeled s-p bonding are bands derived from 4s and 4p arsenic levels and are either bonding with respect to arsenic or bonding with respect to manganese (antibonding with respect to arsenic). The bands labeled s-p antibonding are derived from 4s and 4p manganese levels which are antibonding with respect to manganese or antibonding with respect to arsenic (bonding with respect to manganese). (b) Band model for NiS. The bands labeled s-p bonding (antibonding) are primarily nickel 4s bonding (antibonding) with respect to nickel. These bands necessarily overlap and together correspond to the bands labeled s-p antibonding in (a). Bands corresponding to s-p bonding bands of (a) are not shown in (b), but would lie below the bands shown.

Differences between this model for MnAs and the results of the present calculation for NiS are immediately evident when Figs. 3 and 4 are examined. The major difference is the position of the 4s nickel bands relative to the d bands. Although the 4s nickel and 3p sulfur bands mix, a group of bands in the range -1.8 to -0.8 Ry may be identified as predominately 3p sulfur, containing only very small amounts of nickel s. Bonding and antibonding 3p bands lie in this range. The nickel 4s bonding band begins at -1.43 Ry at Γ and can be seen entering at the bottom of Figs. 3 and 4 near A and exiting at the top after hybridizing with d bands in the middle. The low-lying bands near M are sulfur 3p bands. The 4s antibonding band overlaps the 4s bonding band throughout much of the Brillouin zone, and the two are always degenerate at A. In fact, it is a requirement of group theory for this lattice, that, with respect to the same sublattice, bonding, antibonding bands be degenerate at the zone boundaries $k_z = \pm \pi/c$, whereas they are split at the center of the zone. This may be verified by referring to the symmetrized orbitals given in the Appendix, and is a consequence of time reversal symmetry: There can be no real gaps between the bonding and antibonding bands in the solid. The molecular orbital model has approximate validity only at the center of the zone.[32] However, it is worthwhile to compare relative positions of d bands, which is best done by studying the NiS d bands without hybridization, shown in Fig. 7. Without hybridization, the order of levels at Γ is altered. s and p bands do not interact with the $\Gamma_6^+ d$ levels, so they will not be affected by the addition of nickel s and sulfur p basis functions, while the other levels at Γ are shifted. The additional labels in Fig. 7 are the molecular orbital labels of Goodenough. The + and − symbols indicate bonding and antibonding orbitals with respect to the nickel sublattice. The two-dimensional irreducible representations at Γ contain both e^T bonding and e antibonding functions or vice

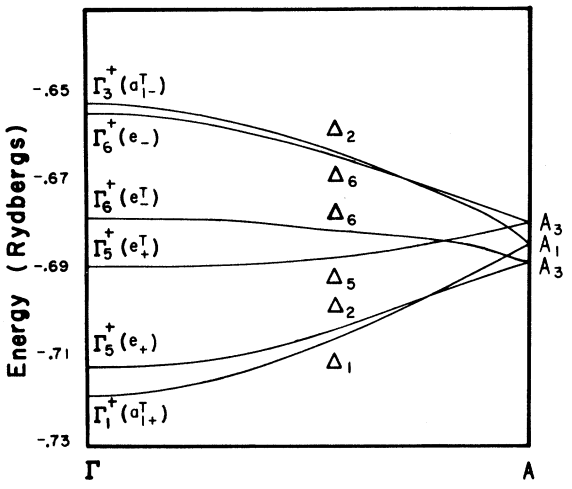

FIG. 7. Energy bands for metallic NiS using d basis functions only.

versa. The labels assigned in Fig. 7 correspond to the largest component, which is usually more than 90%. A schematic diagram for these NiS bands is shown in Fig. 6(b) for comparison with the MnAs diagram, Fig. 6(a). The major difference observed for d bands is overlap of the e and a_1^T bands. As seen from Fig. 3, hybridization with nickel 4s and sulfur 3p bands tends to narrow the e^T band and widen the e band, but does not split away the e band. Thus, the potential used in this calculation does not produce enough crystal field splitting to prevent overlap of all the d bands. The total width of the d bands is about 3.5 eV, but, as anticipated by Goodenough, width of the e^T bands is considerably less, about 0.15 eV.

C. Discussion

Energy bands presented in Figs. 3 and 4 were obtained using nickel 3d and 4s and sulfur 3p orbitals and a crystal potential constructed from neutral atoms. The calculation was not done self-consistently, nor was spin-orbit interaction included in the Hamiltonian. While spin orbit could substantially affect the shape of the Fermi surface by splitting and moving the d bands near the Fermi energy, it should change relative positions of the bands by small amounts only: This will be discussed further in Sec. V. However, self-consistency is a more difficult factor to anticipate, and it is possible that a self-consistent potential would lead to important reordering of bands. Although, in principle, a self-consistent calculation could be carried out for NiS, the present experimental information does not seem to justify the time and expense, which would be substantial. A crude estimate of consistency of this calculation can be made by comparing assumed occupancies of atomic energy levels used to construct the crystal potential with occupancies of corresponding energy bands. This is difficult to do since s, p, and d bands hybridize and mix throughout the zone, making proper correspondence uncertain. From Figs. 3 and 4, the effective configuration in the solid is approximately $\mathrm{Ni}(3d^{7.5}4s^{0.5})\,\mathrm{S}(3p^6)$, i.e., filled 3$p$ bands, whereas the assumed configurations were $\mathrm{Ni}(3d^9 4s^1)\,\mathrm{S}(3p^4)$. Similar results were obtained for ReO_3 with neutral atom potentials[8] and TiO with singly ionized atoms.[33] By examining charge densities within APW spheres the latter case was found to be nearly self-consistent even though band occupancy indicated doubly ionized atoms.

Other uncertainties which are involved include exchange contributions and the importance of additional basis functions, both core and conduction type. To investigate exchange effects, several values of λ were used to obtain energy bands. Figure 5 shows typical results for $\lambda = 0.85$, where the main feature is differences in Fermi energy and Fermi surface caused by the relatively small changes in the exchange potential. Note now the presence of Σ heavy mass holes in the Fermi surface. λ is a convenient parameter for adjusting positions of d bands relative to s bands. Values of λ in the range $\frac{2}{3}$–1 did not alter the order of levels at Γ, so it is not expected that s-d hybridization can be removed by using a slightly different treatment of exchange.

This s-d hybridization, which presents difficulties in Sec. V, could be altered by interaction with other bands not included in this calculation. To investigate this possibility additional core functions were added. All necessary integrals had previously been calculated for s orbitals in the core of nickel, so these were added to the basis set. Energy levels affected at Γ are given in Table I with and without the nickel s core.

TABLE I. Effect of nickel core s functions on energy eigenvalues at Γ. Energies are expressed in Ry. The high-energy state belongs to the nickel 4s antibonding band.

Level	Without core	With core
Γ_3^+	4.910	5.260
Γ_3^+	−0.566	−0.561
Γ_1^+	−0.717	−0.717
Γ_3^+	−1.186	−1.184
Γ_1^+	−1.430	−1.169

Nickel s functions transform as Γ_1^+ or Γ_3^+, and affect only positions of nickel s and d_{z2} bonding and antibonding levels. On the other hand, sulfur s functions transform as Γ_1^+ and Γ_4^- and would alter only the nickel s and d_{z2} bonding levels at Γ if they were included in the basis set. Since the sulfur 3s level is the next highest core level, it is possible that it could substantially change the 4s Γ_1^+ level. To avoid lengthy computations required to include the sulfur s functions, a second-order perturbation estimate was made, based upon first-neighbor interactions only. This estimate indicated that sulfur s functions would contribute approximately the same order corrections as nickel s functions, so that the order of levels at Γ would remain unchanged.

Uncertainty related to contributions from conduction bands is probably larger. Additional s functions on nickel or sulfur would lower the 4s Γ_1^+ level relative to d bands. Sulfur 3d conductions bands may also be important, as noted by Wilson, who reported energy bands for α MnS calculated by the APW method.[34] He found that manganese d bands were pushed down below manganese 4s bands by interaction with sulfur 3d bands. Whether this is the case with NiS is uncertain, since sulfur d functions interact with both s and d bands in the NiAs structure and will lower both energy bands. Nevertheless, it is clear that more accurate calculations for NiS must allow for this possibility either by inclusion of more tight-binding functions or addition of plane waves to the basis set.

D. Density of States and Optical Properties

In Fig. 8 is shown the density of states for energy bands of Figs. 3 and 4 ($\lambda = 1$), which was obtained using a grid of 327 points within $\frac{1}{24}$ of the Brillouin zone. The Fermi energy is -0.616 Ry. This density of states is characterized by two strong peaks in the d bands, one just above and the other below the Fermi energy. A broad peak below the Fermi energy corresponds to s and p bands. The strong, sharp peak just below the Fermi energy may be traced to the lower T_2, T_3 bands (Fig. 4) and corresponding bands along other axes. These bands are the narrow (0.14 eV) e^T bands described by Goodenough,[30] which are possibly responsible for the magnetic properties of transition metal compounds which crystallize in the NiAs structure. A density of states characterized by a Fermi energy lying in a minimum between two d band maxima is considered by some to be favorable to antiferromagnetism.[31,35]

The narrow d bands and large peaks in density of states near the Fermi energy suggest that there should be substantial structure in optical reflectivity of NiS in the infrared region. For the purpose of understanding this structure, and in hopes of stimulating experimental investigations, selection rules and transition energies have been worked out for the band structure presented here. Selection rules were obtained by standard group theoretic techniques. Transition energies were chosen for transitions likely to exhibit structure in the reflectivity: Those for which the joint den-

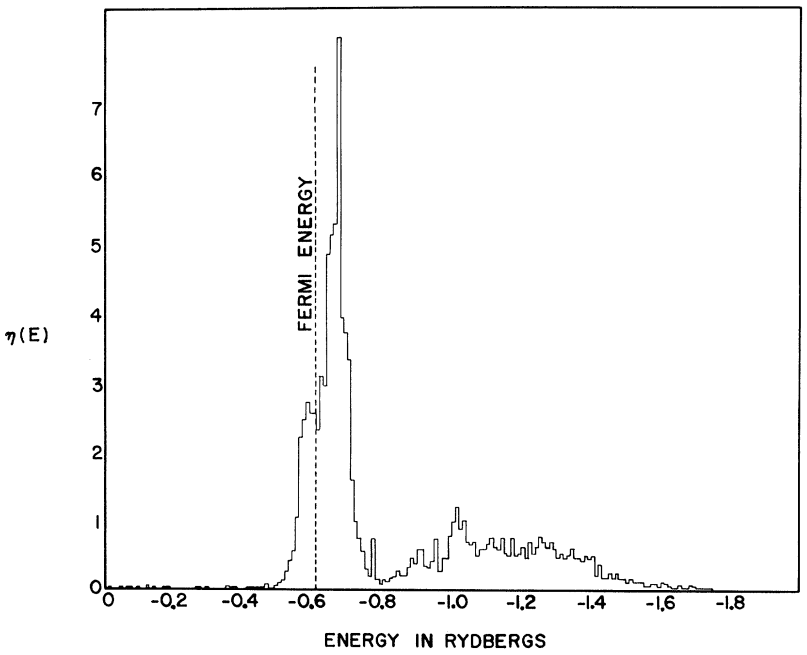

FIG. 8. Density of states for metallic NiS.

sity-of-states function is large. This was done by examining energy bands shown in Figs. 3 and 4. A list of important electric dipole transitions below 10 eV, along with selection rules for light polarized parallel or perpendicular to the Z axis is given in Table II.

V. METAL-TO-SEMICONDUCTOR TRANSITION

The metal-to-semiconductor transition in NiS has been attributed to antiferromagnetic ordering of magnetic moments of nickel atoms.[2] It is interesting to examine the band structure of the metallic phase of NiS to see whether conditions are favorable for antiferromagnetism. If so, a spin-polarized calculation[6] using lattice constants for the semiconducting phase might be successful in explaining the semiconducting behavior below the Néel temperature. According to simple band theory it is necessary that the spin splitting of the bands leave completely filled or completely empty bands. This is most easily accomplished when an exactly half-filled band, which does not overlap any other band, is split in half. This would be the case when bandwidths are small compared to crystal field splittings which in turn are small compared with spin splitting, which appears to be the case with NiO. Energy bands obtained here do not satisfy these conditions. First, the d bandwidths are larger than the crystal field splittings, causing bands to overlap in a complicated way. Second, the 4s bands overlap all the d bands, and, since they are so wide, will probably overlap all d bands after a spin splitting is introduced, since it is not likely to be larger than the bandwidth of the combined 4s bonding, antibonding bands. Thus it is not easy to visualize a model band structure which would be split correctly by antiferromagnetic alignment of spins to give a real gap in the density of states.

In order to construct such a model from results of the present calculations it is essential to consider spin-orbit effects. This is done crudely by relabeling energy levels according to the double group notations and reconnecting them as required by symmetry, as shown in Fig. 9. No spin-orbit splittings are shown: Results from band calculations of fcc nickel suggest that these splittings would be less than 0.2 eV. Degeneracies will be removed whenever two different double-group irreducible representations appear as labels at the same point, except for those which are required to be degenerate by time reversal symmetry, e.g., A_4+A_5. By arbitrarily moving levels at Γ, A, and L above or below the Fermi energy and introducing a spin-orbit splitting of A_6 from A_4+A_5, it might be possible to obtain a band structure favorable toward formation of an antiferromagnetic semiconductor. However, due to relative positions of s and d levels and the resulting hybridization, it is very difficult, if not impossible, to find a way to make minor adjustments of these energy bands that will lead to a real gap in the density of states after the energy bands are split by introducing the magnetic Brillouin zone. For reasonable values of spin splittings it is not possible to obtain a real gap even by arbitrarily moving levels by amounts of the order of widths of the d bands.

On the other hand, if the 4s band is first lifted above the 3d bands by an amount large compared to the spin splitting, the 3d bands are connected differently, and it is then possible to obtain a band structure (perhaps not a very probable one) in which a gap can appear. Since d bands of the same spin but different symmetries will presumably still overlap after the spin splitting is introduced, the largest band gap which can occur must be less than the maximum spin-orbit splitting, about 0.2 eV, which is not inconsistent with the observed activation energy of semiconducting NiS, 0.12 eV. Without splitting apart of the d bands by spin-orbit interactions there can be no gaps introduced by spin splittings, even when the order of s and d bands is altered.

TABLE II. Some low-energy electric dipole transitions for metallic NiS as deduced from the band structure of Figs. 3 and 4. Light polarized parallel to the c axis transforms like Γ_2^-, while light polarized perpendicular to the c axis transforms like Γ_6^-. Only direct transitions are considered here, and no selection rules relying on time reversal symmetry are included. All $+\rightarrow+$ or $-\rightarrow-$ transitions such as $M_1^+\rightarrow M_2^+$ or $\Gamma_3^-\rightarrow\Gamma_6^-$, etc., are forbidden.

Transition	Energy (eV)	Selection rules $\parallel c$ axis	Selection rules $\perp c$ axis
A_1-A_1	9.4	Yes	No
Σ_3-Σ_3	7.9	No	Yes
Σ_3-Σ_4	8.4	No	No
$R_{1,3}$-$R_{1,3}$	1.52	Yes	Yes
U_2-U_2	1.63	Yes	No
$R_{1,3}$-$R_{2,4}$	0.32	No	Yes
$R_{1,3}$-$R_{2,4}$	1.27	No	Yes
$R_{1,3}$-$R_{1,3}$	0.98	Yes	Yes
K_5-K_6	0.44	No	Yes
K_1-K_6	1.20	No	Yes
Σ_3-Σ_4	1.74	No	No
Σ_3-Σ_2	0.87	No	Yes
T_2-T_1	1.30	No	No
T_3-T_1	0.10	Yes	No
S_1-S_1	0.32	Yes	Yes
S_1-S_1	1.03	Yes	Yes
S_1-S_1	1.36	Yes	Yes
S_1-S_1	1.57	Yes	Yes

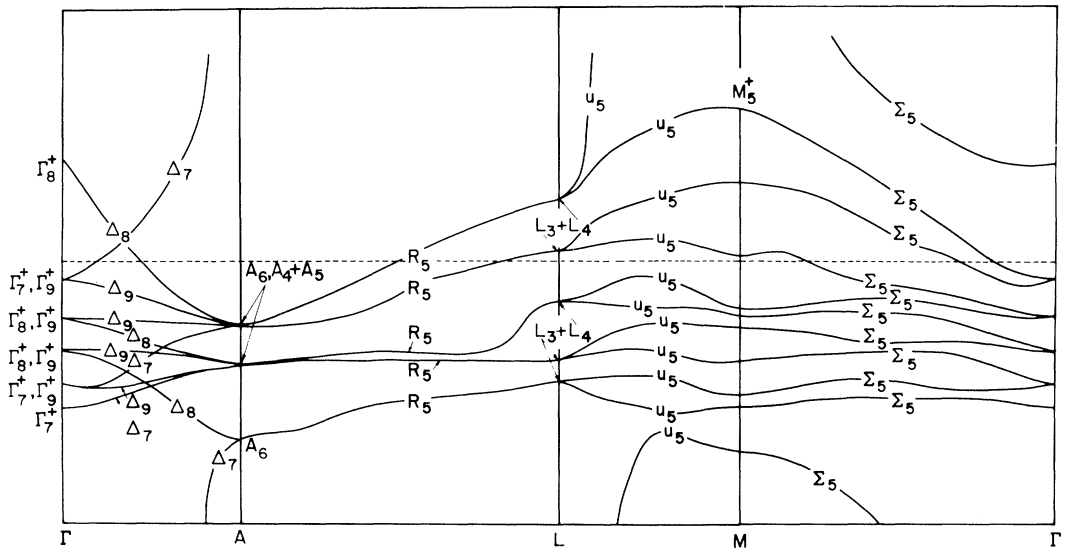

FIG. 9. Energy bands for metallic NiS labeled according to double-group irreducible representations.

Thus, about the only possibility of understanding the phase transition in NiS in terms of a spin-polarized model and the band structure presented here requires reordering of s and d levels and invoking both spin splitting and spin-orbit splitting of d bands. If this model is correct, the NiS transition might in fact be a semimetal-to-semiconductor transition.

However, if the present band structure is correct as far as order of s and d levels, crystal field splittings, and bandwidths, it may be necessary to take another point of view to understand the phase transition: that the transition is a collective-to-localized one, in other words, a Mott transition.[36] In this case, magnetic order would not be necessary, but could be attributed to localization of the d electrons.

VI. CONCLUSION

In this paper the energy bands of NiS have been examined by using a tight-binding method. Although the method has been applied with greater rigor than usual, it is possible that further refinements will alter the band structure obtained here. Additional tight-binding basis functions may be needed, and perhaps a better treatment of exchange. The former could be added with sufficient labor at this time, but the latter improvement would need some experimental guidelines which are not available at present. Probably the most important consideration for further refinement is improvement of the crystal potential toward self-consistency. Conclusions reached here about the band structure of NiS are based upon a neutral atom crystal potential and the crystal field splittings, bandwidths, and band overlaps associated with it. Although a self-consistent calculation starting from the present band structure could conceivably produce changes in all three of these band properties, it is not possible to anticipate whether they are substantial enough to alter conclusions reached here.

The principal results of this calculation may be summarized as follows:

(a) It has been demonstrated that a straightforward application of the tight-binding method is possible for a fairly complicated transition metal compound (two molecules per unit cell, and a hexagonal nonsymmorphic space group).

(b) The nickel $3d$ bands of metallic NiS are about 3.5 eV wide and overlapped by and hybridized with the nickel $4s$ band.

(c) The Fermi surface is complicated: Conductivity is due to both s and d electrons and holes.

(d) An abundance of low-energy electric dipole transitions should be observed in the infrared reflectivity of NiS.

(e) The density of states may be favorable toward the formation of antiferromagnetic order, but the addition of spin polarization to the present calculation is not likely to result in a semiconducting band structure for NiS.

ACKNOWLEDGMENTS

The authors would like to thank the Computer Research Center of Louisiana State University for assistance with this work. Thanks are also due to Professor N. Kestner of the Chemistry Depart-

ment for providing the authors with a computer program to evaluate kinetic-energy integrals, and to Professor J. Callaway for many useful conversations.

APPENDIX

Presented here are symmetrized combinations of atomic orbitals for the NiAs structure for s, p, and d functions on nickel sites and s and p functions on arsenic sites. Subscripts 1 and 2 refer to nickel sites $\vec{\tau}_1$ and $\vec{\tau}_2$; 3 and 4 refer to arsenic (sulfur in NiS) sites $\vec{\tau}_3$ and $\vec{\tau}_4$. Symmetrized functions were obtained using projection operators and matrix elements of irreducible representations given in Ref. 26. To simplify these lists, the following notations are used in addition to the subscripts: x^2 means x^2-y^2 and z^2 means $3z^2-r^2$; xy_1 means $(xy)_1$, etc. The first column below is the dimension of the irreducible representation which is labeled in the second column, followed by the symmetrized combinations of orbitals. The factor A is $\exp(-i\pi k_z)$. For multidimensional representations, functions which transform like different rows are separated by commas, or indicated by ± signs. The order of rows is the same for different s, p, or d groups separated by semicolons. In some cases it may be possible to choose real basis functions instead of the complex ones listed here.

1 Γ_1^+ S_1+S_2; S_3+S_4; $z_1^2+z_2^2$,

1 Γ_2^- z_1+z_2; z_3+z_4,

1 Γ_3^+ S_1-S_2; z_3-z_4; $z_1^2-z_2^2$,

1 Γ_4^- S_3-S_4; z_1-z_2,

2 Γ_5^+ $x_3-x_4\mp i(y_3-y_4)$; $xy_1+xy_2\mp i(x_1^2+x_2^2)$; $yz_1-yz_2\mp i(xz_1-xz_2)$,

2 Γ_5^- $x_1-x_2\mp i(y_1-y_2)$,

2 Γ_6^+ $xy_1-xy_2\pm i(x_1^2-x_2^2)$; $yz_1+yz_2\mp i(xz_1+xz_2)$,

2 Γ_6^- $x_3+x_4\pm i(y_3+y_4)$; $x_1+x_2\pm i(y_1+y_2)$,

1 K_1 S_1+S_2; S_3+S_4; $z_1^2+z_2^2$,

1 K_2 S_1-S_2; z_3-z_4; $z_1^2-z_2^2$,

1 K_3 S_3-S_4; z_1-z_2,

1 K_4 z_1+z_2; z_3+z_4,

2 K_5 $x_1+x_2\mp i(y_1+y_2)$; $x_3\pm iy_3$; $xy_1+xy_2\mp i(x_1^2+x_2^2)$; $yz_1-yz_2\pm(xz_1-xz_2)$,

2 K_6 $xy_1-xy_2\mp i(x_1^2-x_2^2)$; $yz_1+yz_2\pm i(xz_1+xz_2)$,

1 Δ_1 $S_1+\alpha S_2$; $z_1^2+\alpha z_2^2$,

1 Δ_2 $S_1-\alpha S_2$; $S_3-\alpha S_4$; $z_1-\alpha z_2$; $z_3-\alpha z_4$; $z_1^2-\alpha z_2^2$,

2 Δ_5 $x_1-\alpha x_2\mp i(y_1-\alpha y_2)$; $x_3-\alpha x_4\mp i(y_3-y_4)$; $xy_1+\alpha xy_2\mp i(x_1^2+\alpha x_2^2)$; $yz_1-\alpha yz_2\pm i(xz_1-\alpha xz_2)$,

2 Δ_6 $x_1+\alpha x_2\pm i(y_1+\alpha y_2)$; $x_3+\alpha x_4\pm i(y_3+\alpha y_4)$; $xy_1-\alpha xy_2\pm i(x_1^2-\alpha x_2^2)$; $yz_1+\alpha yz_2\mp i(xz_1+\alpha xz_2)$,

2 A_1 $S_1\pm iS_2$; $S_3\pm iS_4$; $z_1\mp iz_2$; $z_3\mp iz_4$; $z_1^2\mp iz_2^2$,

4 A_3 $x_1+y_2\pm i(x_2-y_1)$, $x_1-y_2\pm i(x_2+y_1)$; $x_3+y_4\pm i(x_4-y_3)$, $x_3-y_4\pm i(x_4+y_4)$; $xy_1-x_2^2\mp i(xy_2+x_1^2)$, $xy_1+x_2^2\mp i(xy_2-x_1^2)$; $yz_1-xz_2\pm i(yz_2+xz_1)$, $yz_1+xz_2\pm i(yz_2-xz_1)$,

2 H_1 S_1+S_2, S_1-S_2; S_3, S_4; z_1-z_2, z_1+z_2; $z_1^2+z_2^2$, $z_1^2-z_2^2$,

2 H_2 $x_1+x_2\mp i(y_1+y_2)$, x_3-iy_3, x_4-iy_4; $xy_1\pm xy_2+i(x_2^2\pm x_1^2)$; $yz_1\mp yz_2+i(xz_2\mp xz_1)$,

1 P_1 $S_1+\alpha S_2$; $S_3+\alpha S_4$; $z_1+\alpha z_2$; $z_3+\alpha z_4$; $z_1^2+\alpha z_2^2$,

1 P_2 $S_1-\alpha S_2$; $S_3-\alpha S_4$; $z_1-\alpha z_2$; $z_3-\alpha z_4$; $z_1^2-\alpha z_2^2$,

2 P_3 x_1-iy_1, x_2-iy_2; x_3-iy_3, x_4-iy_4; $xy_1+ix_1^2$, $xy_2+ix_2^2$; yz_1-ixz_1, yz_2-ixz_2,

1 Σ_1 S_1+S_2; S_3; S_4; x_1+x_2; x_3; x_4; z_1-z_2; $x_1^2+x_2^2$; xz_1-xz_2; $z_1^2+z_2^2$,

1 Σ_2 y_1-y_2; z_1+z_2; xy_1-xy_2; yz_1+yz_2,

1 Σ_3 S_1-S_2; x_1-x_2; z_3; z_4; $x_1^2-x_2^2$; $z_1^2-z_2^2$,

1 Σ_4 y_1+y_2; y_3; y_4; xy_1+xy_2; yz_1-yz_2,

1 M_1^+ S_1+S_2; S_3+S_4; x_3-x_4; $x_1^2-x_2^2$; xz_1-xz_2; $z_1^2+z_2^2$,

1 M_1^- y_1-y_2,

1 M_2^+ x_3+x_4; xy_1-xy_2; yz_1+yz_2,

1 M_2^- S_3-S_4; x_1+x_2; z_1-z_2,

1 M_3^+ S_1-S_2; z_3-z_4; $x_1^2-x_2^2$; xz_1+xz_2; $z_1^2-z_2^2$,

1 M_3^- y_1+y_2; y_3+y_4,

1 M_4^+ y_3-y_4; xy_1+xy_2; yz_1-yz_2,

1 M_4^- x_1-x_2; z_1+z_2; z_3+z_4,

1 T_1, T_1' S_1+S_2; S_3+S_4; x_3-x_4; y_3+y_4; $x_1^2+x_2^2$;

$xz_1 - xz_2;\ z_1^2 + z_2^2,$

1 T_2, T_2' $S_1 - S_2;\ y_1 - y_2;\ z_3 - z_4;$
$x_1^2 + x_2^2;\ xz_1 + xz_2;\ z_1^2 - z_2^2,$

1 T_3, T_3' $x_1 - x_2;\ z_1 + z_2;\ z_3 + z_4;$
$xy_1 - xy_2;\ yz_1 + yz_2,$

1 T_4, T_4' $S_3 - S_4;\ x_1 + x_2;\ x_3 + x_4;\ y_3 - y_4;\ z_1 - z_2;$
$xy_1 + xy_2;\ yz_1 - yz_2,$

1 R_1 $S_1 + S_2;\ S_3;\ S_4;$
$x_1 + x_2;\ x_3;\ x_4;\ z_1 - z_2;\ x_1^2 + x_2^2;$
$xz_1 - xz_2;\ z_1^2 + z_2^2,$

1 R_2 $y_1 - y_2;\ xy_1 - xy_2;\ yz_1 + yz_2,$

1 R_3 $S_1 - S_2;\ x_1 - x_2;\ y_1 + y_2;$
$z_1 + z_2;\ z_3;\ z_4;\ x_1^2 - x_2^2;$
$xz_1 + xz_2;\ z_1^2 - z_2^2,$

1 R_4 $y_3;\ y_4;\ xy_1 + xy_2;\ yz_1 - yz_2,$

2 L_1 $S_1 \pm S_2;\ S_3,\ S_4;\ x_1 \pm x_2;$
$x_3,\ x_4;\ z_1 \pm z_2;\ z_3,\ z_4;$
$x_1^2 \pm x_2^2;\ xz_1 \mp xz_2;\ z_1^2 \pm z_2^2,$

2 L_2 $y_1 \pm y_2;\ y_3,\ y_4;\ xy_1 \pm xy_2;\ yz_1 \mp yz_2,$

1 U_1 $S_1 + \alpha S_2;\ S_3 + \alpha S_4;$
$x_1 - \alpha x_2;\ x_3 - \alpha x_4;\ z_1 + \alpha z_2;$
$z_3 + \alpha z_4;\ x_1^2 + \alpha x_2^2;\ xz_1 - \alpha xz_2;\ z_1^2 + \alpha z_2^2,$

1 U_2 $S_1 - \alpha S_2;\ S_3 - \alpha S_4;$
$x_1 + \alpha x_2;\ x_3 + \alpha x_4;\ z_1 - \alpha z_2;$
$z_3 - \alpha z_4;\ xy_1 - \alpha xy_2;\ xz_1 + \alpha xz_2;\ z_1^2 - \alpha z_2^2,$

1 U_3 $y_1 + \alpha y_2;\ y_3 + \alpha y_4;\ xy_1 - \alpha xy_2;\ yz_1 + \alpha yz_2,$

1 U_4 $y_1 - \alpha y_2;\ y_3 - \alpha y_4;\ xy_1 + \alpha xy_2;\ yz_1 - \alpha yz_2.$

---

†Work supported by the U.S. Air Force Office of Scientific Research under Grant No. AFOSR 68-1565.

*National Science Foundation Trainee. Present Address: IBM, Baton Rouge, La.

[1]R. W. G. Wyckoff, *Crystal Structures* (Interscience, New York, 1963).

[2]D. Adler, in *Solid State Physics*, edited by F. Seitz, D. Turnbull, and H. Ehrenreich (Academic, New York, 1968), Vol. 21, p. 1.

[3]D. Adler and J. Feinleib, J. Appl. Phys. 40, 1586 (1969); J. Feinleib and D. Adler, Phys. Rev. Letters 21, 1010 (1968).

[4]J. B. Goodenough, J. Appl. Phys. 39, 403 (1968).

[5]T. M. Wilson, J. Quantum Chem. 52, 269 (1969).

[6]J. C. Slater, J. Appl. Phys. 39, 767 (1968).

[7]J. T. Sparks and T. Komoto, Phys. Letters 25A, 393 (1967).

[8]L. F. Mattheis, Phys. Rev. 181, 987 (1969).

[9]J. T. Sparks and T. Komoto, Rev. Mod. Phys. 40, 752 (1968).

[10]J. T. Sparks and T. Komoto, J. Appl. Phys. 34, 1191 (1963).

[11]J. T. Sparks and T. Komoto, J. Appl. Phys. 39, 715 (1968).

[12]I. Tsubokawa, J. Phys. Soc. Japan 13, 1432 (1958).

[13]J. T. Sparks and T. Komoto, J. Phys. Radium 25, 567 (1964).

[14]S. Anzai and K. Ozawa, J. Phys. Soc. Japan 24, 271 (1968).

[15]F. A. Smith and J. T. Sparks, J. Appl. Phys. 40, 1332 (1969).

[16]J. Callaway, *Energy Band Theory* (Academic, New York, 1964).

[17]J. C. Slater and G. F. Koster, Phys. Rev. 94, 1498 (1954).

[18]A. Nussbaum, in Ref. 2, Vol. 18, p. 165.

[19]E. E. Lafon and C. C. Lin, Phys. Rev. 152, 579 (1966).

[20]J. M. Tyler, T. E. Norwood, and J. L. Fry, Phys. Rev. B 1, 297 (1970).

[21]M. Kotani, A. Amemiya, E. Ishiguro, and T. Kimura, *Tables of Molecular Integrals* (Maruzen Co. Ltd., Tokyo, Japan, 1963).

[22]I. Shavitt, in *Methods in Computational Physics*, edited by B. Adler, S. Fernbach, and M. Rotenberg (Academic, New York, 1963), Vol. 2, p. 1.

[23]E. Clementi, *Tables of Atomic Wave Functions* (International Business Machines Corp., San Jose, Calif. 1965).

[24]J. C. Slater, Phys. Rev. 81, 385 (1951); see also J. C. Slater, T. M. Wilson, and J. H. Wood, Phys. Rev. 179, 28 (1969).

[25]P. P. Ewald, Ann. Physik 64, 253 (1921).

[26]J. C. Slater, *Quantum Theory of Molecules and Solids* (McGraw-Hill, New York, 1965), Vol. 2.

[27]C. Herring, J. Franklin Inst. 233, 525 (1942).

[28]J. Callaway and H. M. Zhang, Phys. Rev. B 1, 305 (1970).

[29]J. Q. Bartling, Ph. D. thesis, University of California, Riverside, Calif., 1969 (unpublished).

[30]J. B. Goodenough and J. A. Kafalas, Phys. Rev. 157, 389 (1967); N. Menyak, J. A. Kafalas, D. Dwight, and J. B. Goodenough, *ibid.* 177, 942 (1969).

[31]J. B. Goodenough, *Magnetism and the Chemical Bond* (Interscience, New York, 1963); in *Magnetism*, edited by G. T. Rado and H. Suhl (Academic, New York, 1963), Vol. 3 p. 1.

[32]For a discussion of the relation between molecular orbital theory and tight-binding theory as applied to ReO_3, see Ref. 8. A more complete tight-binding formalism for ReO_3 has been given by J. M. Honig, J. O. Dimmock, and W. H. Kleiner, J. Chem. Phys. 50, 5232 (1969).

[33]V. Ern and A. C. Switendick, Phys. Rev. 137, A1927 (1965).

[34]T. M. Wilson, Intern. J. Quantum Chem. SIII, 757 (1970).

[35]J. Yamashita, S. Asano, and S. Wakoh, J. Appl. Phys. 39, 1274 (1968).

[36]N. F. Mott, Proc. Phys. Soc. (London) A62, 416 (1949).